Title:

In silico description of the direct inhibition mechanism of endothelial lipase by ANGPTL3

Linda Montavoci[1,2,†], Omar Ben Mariem[1,†], Simona Saporiti[3], Tommaso Laurenzi[1], Luca Palazzolo[1], Alice Ossoli[4], Uliano Guerrini[1], Laura Calabresi[4], and Ivano Eberini[5,*]

[1] Dipartimento di Scienze Farmacologiche e Biomolecolari, Università degli Studi di Milano, Milan, Italy

[2] Dipartimento di Scienze della Salute, Università degli Studi di Milano, Milan, Italy

[3] Analytical Excellence and Program Management, Merck Serono S.p.A., Rome, Italy

[4] Centro E. Grossi Paoletti, Dipartimento di Scienze Farmacologiche e Biomolecolari, Università degli Studi di Milano, Milan, Italy

[5] Dipartimento di Scienze Farmacologiche e Biomolecolari & DSRC, Università degli Studi di Milano, Milan, Italy

† These authors contributed equally

* Corresponding author: ivano.eberini@unimi.it, via Giuseppe Balzaretti, 9 – 20133 - Milan, Italy

# SUPPLEMENTARY MATERIAL
Figures
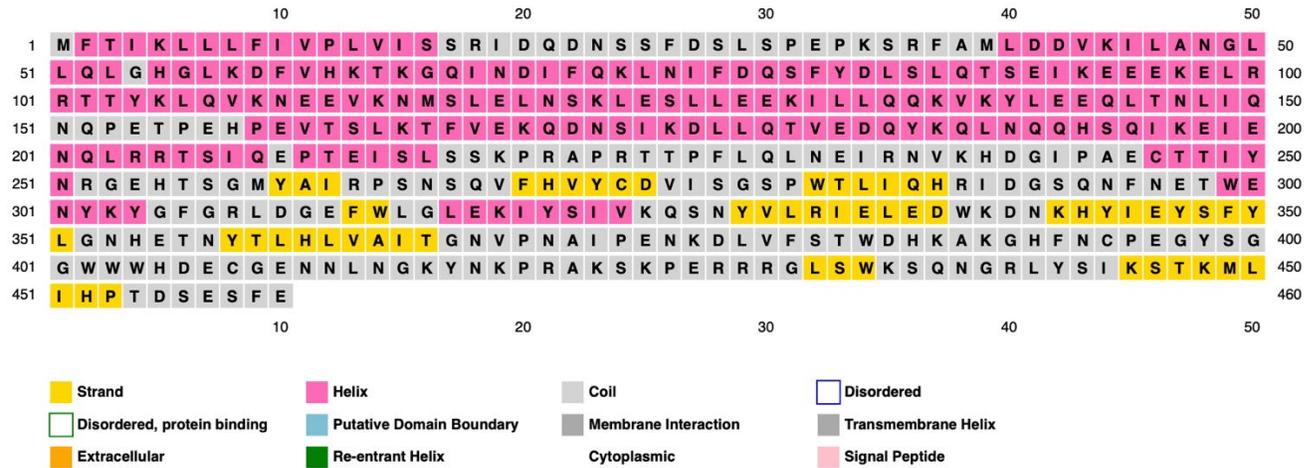
Supplementary figure 1: Secondary structure prediction of ANGPTL3
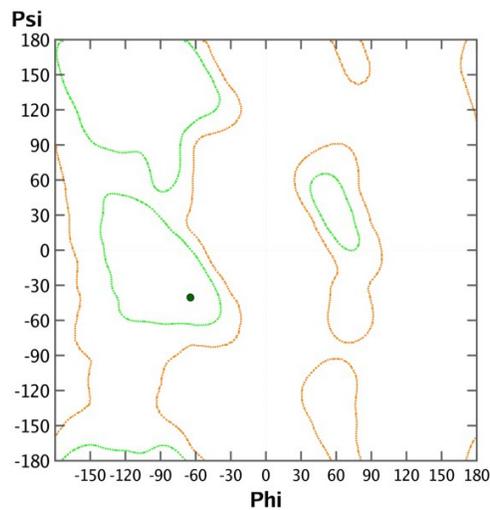
**Supplementary figure 2**: Ramachandran Plot of ANGPTL3 models obtained with CCBuilder before MD simulations. The phi-psi values for all residues are ideal and identical, resulting in a plot apparently containing one single point.
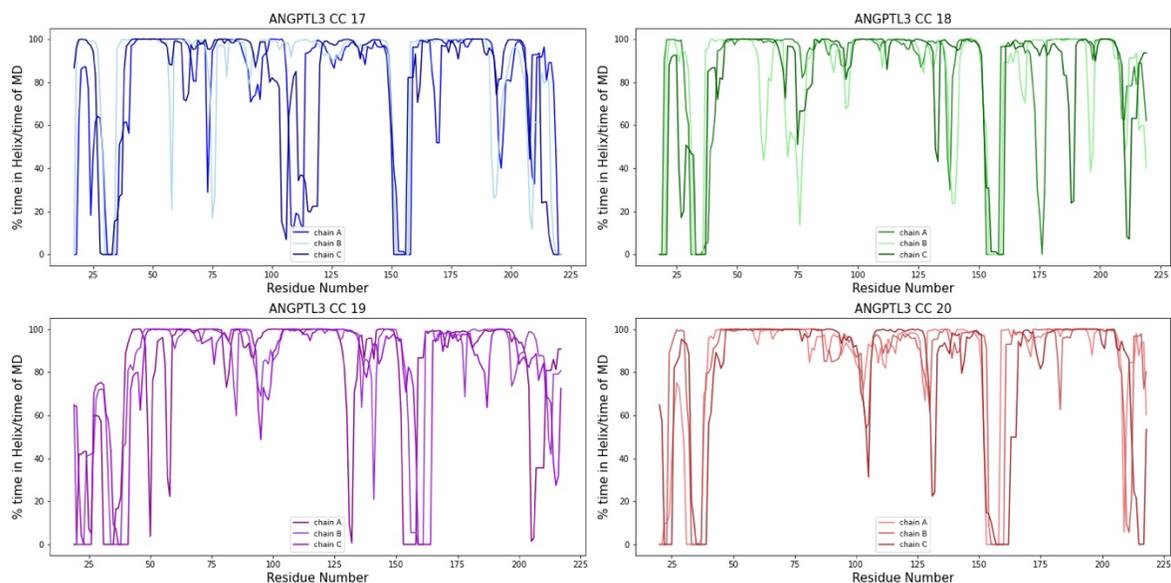
Supplementary figure 3: Time percentage in α-helix of each residue of ANGPTL3 models during MD simulations.
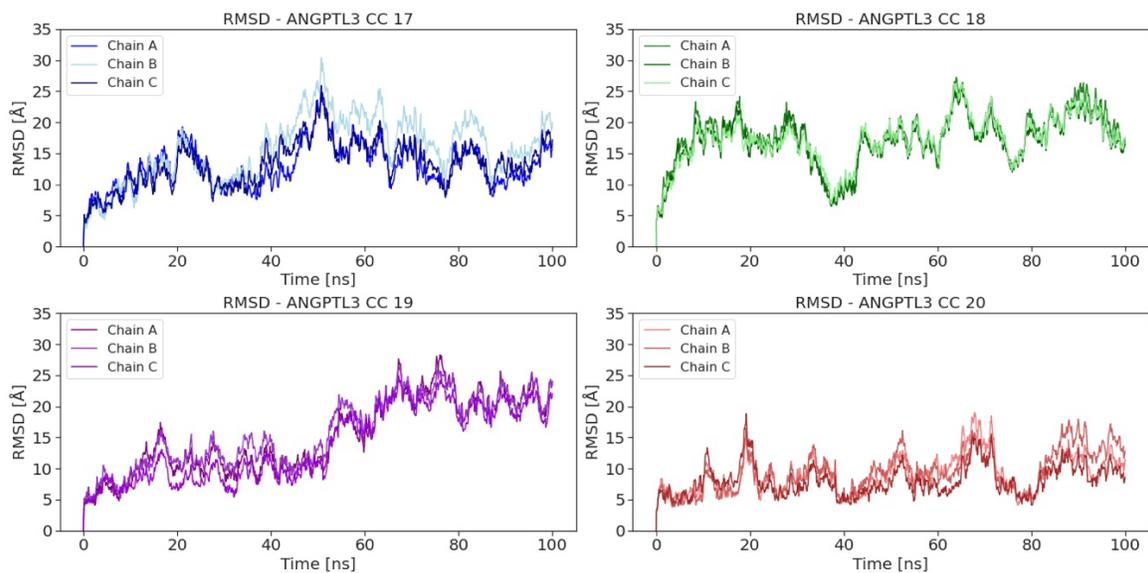
Supplementary figure 4: RMSD during MD simulation of ANGPTL3 models.
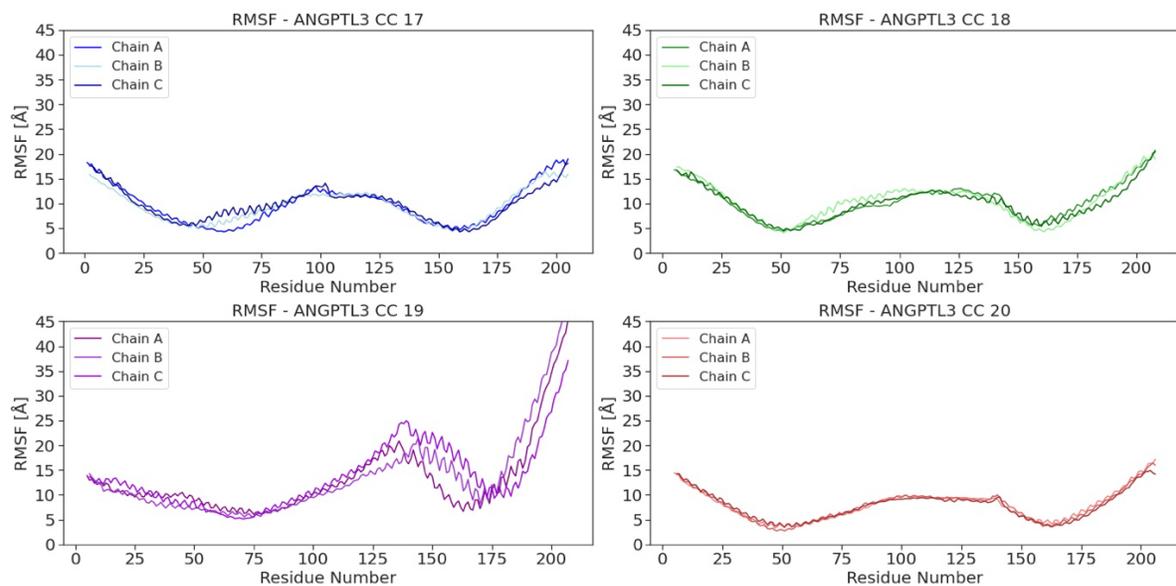
Supplementary figure 5: RMSF during MD simulation of ANGPTL3 models
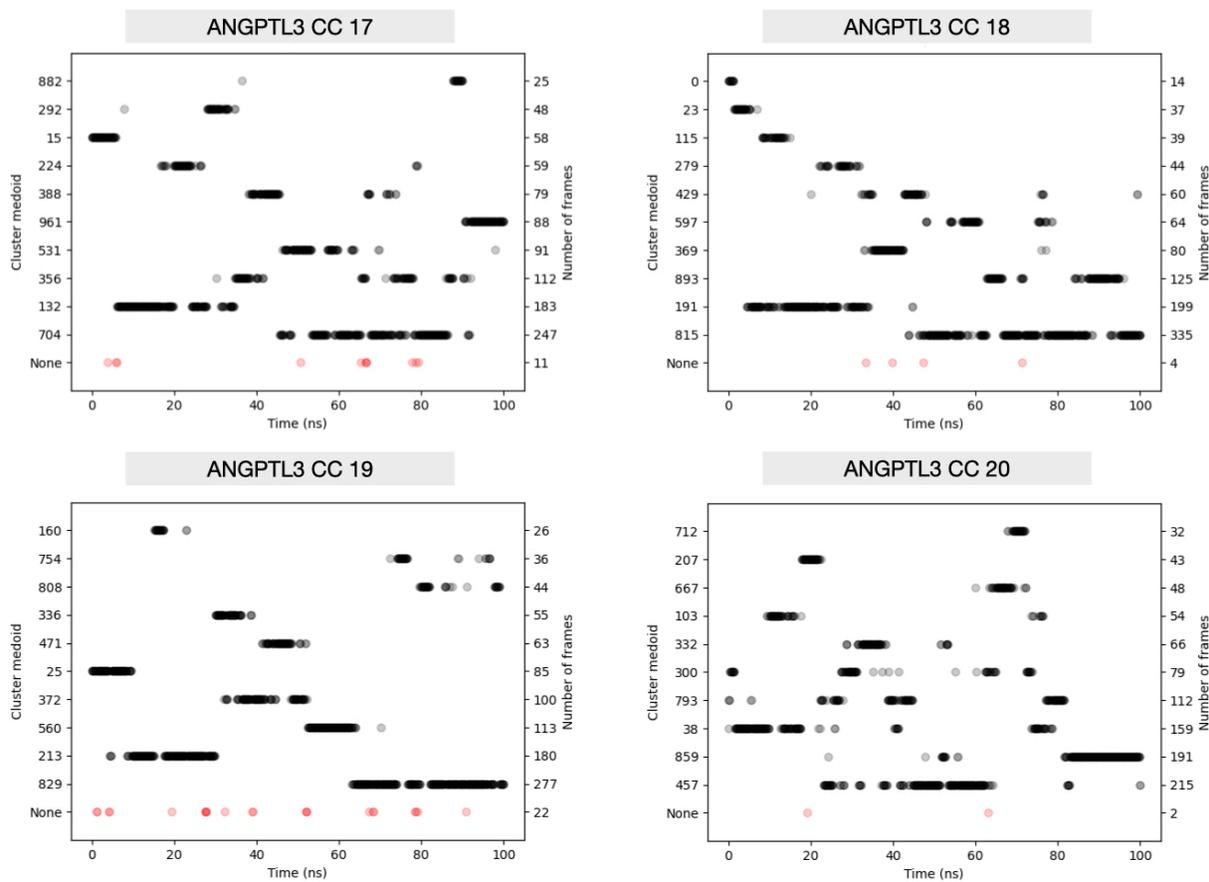
Supplementary figure 6: Cluster analysis performed during MD simulations.
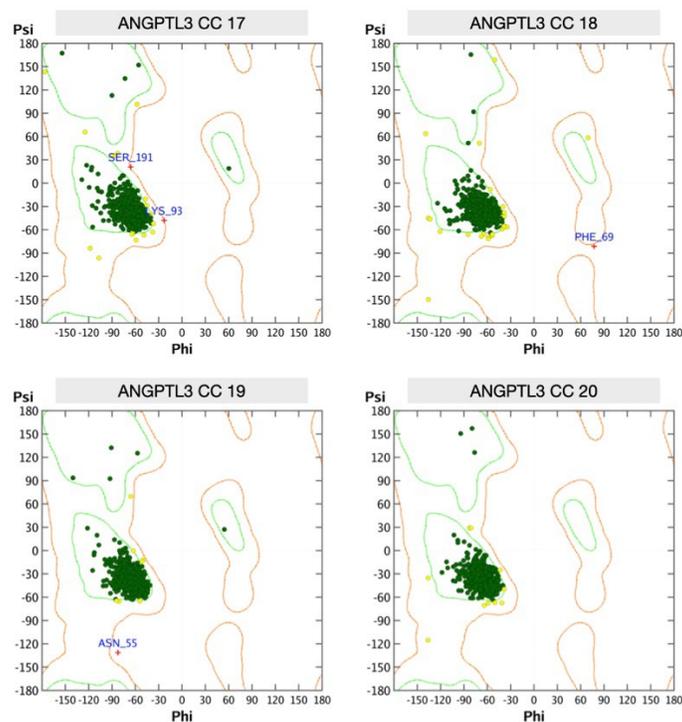
Supplementary figure 7: Ramachandran Plot of ANGPTL3 medoids from the most populated clusters after MD simulation
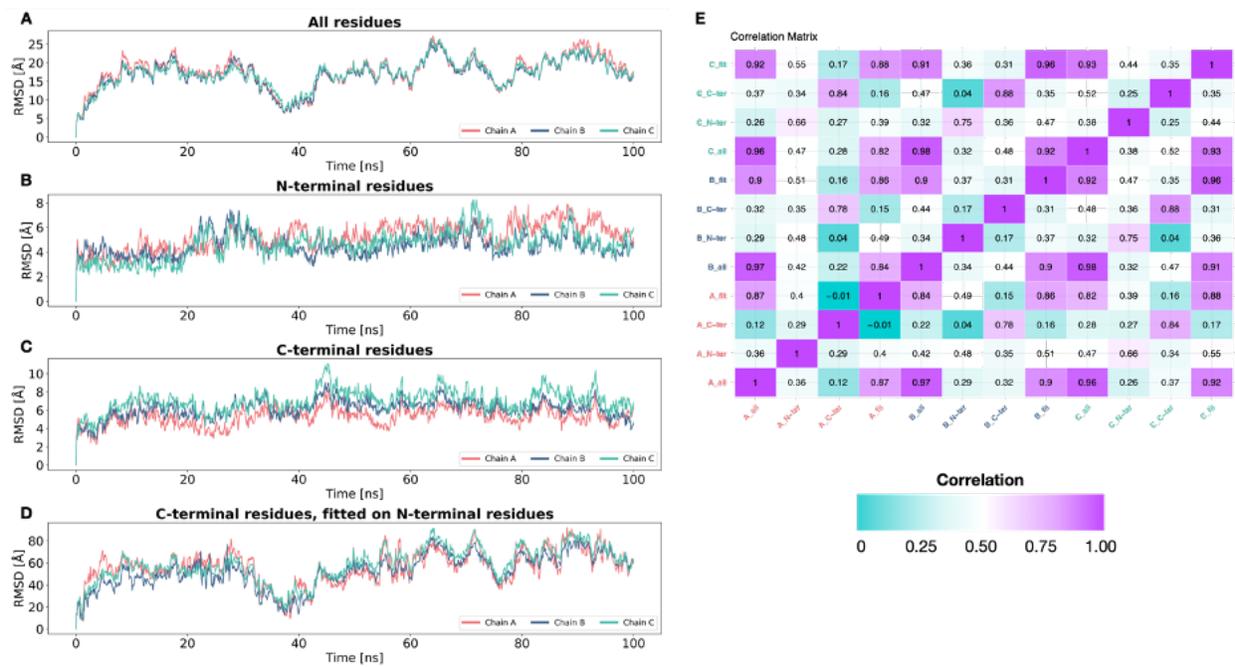
Supplementary figure 8: ANGPTL3 RMSD profiles, referring to Fig. 2, with more appropriate scales on the y-axis for each profile. A) RMSD profile calculated on the overall structure. B)

RMSD profile calculated on the N-terminal portion (residues 18-135). C) RMSD profile calculated on the C-terminal portion (residues 136-221). D) RMSD profile calculated on the C-terminal portion fol-lowing the superposition over the N-terminal portion. This series of calculations highlights that the fluctuation of overall RMSD profile can be attributed to the significant mobility of the final 86 residues subsequent to the bend. E) Correlation matrix calculated between RMSD profiles reported in Fig. 2. It is possible to appreciate the concordant behavior of the chains as well as the strong relationship between overall RMSD values and C-terminal fluctuations.
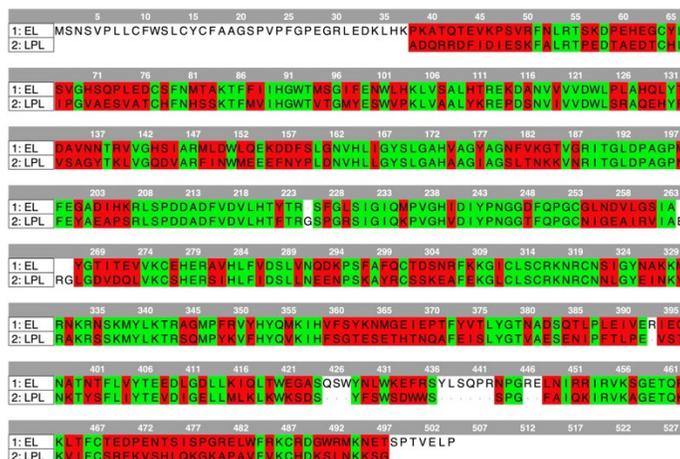
Supplementary figure 9: Alignment between query sequence of EL and template sequence of LPL. The residues are colored by identity, where red indicates different residues and green means same residues.
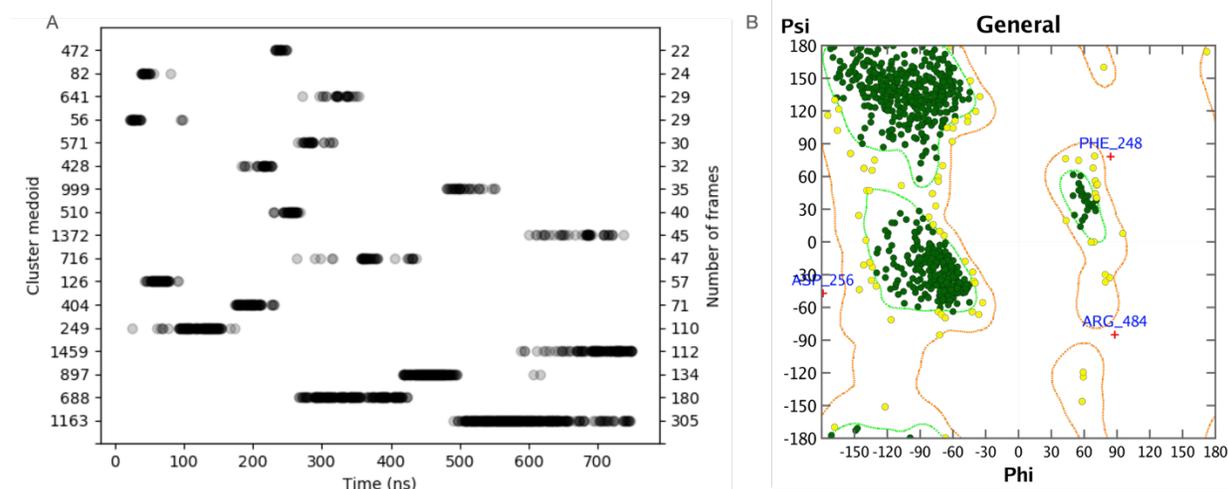
Supplementary figure 10: Cluster analysis (A) and Ramachandran Plot (B) of MD simulation of EL

6

POSE #1 - MOE

ANGPTL3-EL	%
C PRO 143 - D LYS 352	
C GLU 144 - D THR 395	
C SER 150 - D ARG 448	
C GLU 147 - D LYS 352	
B ILE 136 - D ARG 312	
C SER 150 - D ASN 445	
C GLU 147 - D ARG 448	
B GLN 139 - D ARG 312	
B PRO 140 - D LYS 459	
C GLN 158 - D GLU 443	
B GLU 144 - D ARG 450	
B GLU 129 - D ARG 330	
B GLU 147 - D ARG 488	
B GLU 144 - D MET 489	
B GLU 141 - D ARG 450	
C GLU 144 - D LYS 352	
C GLU 147 - D ARG 450	
B GLU 141 - D LYS 459	
B GLU 144 - D LYS 459	

POSE #2 - MOE

| ANGPTL3-EL	%
B GLU 141 - D ARG 450	
A LYS 110 - D ASP 203	
B GLU 130 - D ARG 302	
A GLU 117 - D ARG 207	
C GLN 158 - D GLU 443	
C GLU 144 - D THR 395	
C GLU 144 - D ARG 450	
B THR 133 - D ARG 302	
B GLN 137 - D ILE 307	
B ASN 134 - D ARG 302	
C SER 150 - D ASN 445	
C SER 150 - D ARG 448	
C GLU 147 - D HIS 354	
C GLU 147 - D ARG 450	
B GLU 144 - D MET 489	
B GLU 144 - D LYS 459	
C GLU 144 - D LYS 352	
C GLU 147 - D ARG 448	
B GLU 141 - D LYS 459	

POSE #3 - MOE

ANGPTL3-EL	%
B GLU 112 - E THR 395	
A GLU 106 - E GLU 443	
B GLN 122 - E GLN 392	
B GLN 122 - E ASN 360	
B GLN 122 - E ASN 393	
C GLU 144 - D LYS 305	
B LYS 118 - E SER 357	
C GLU 144 - D ARG 302	
C GLU 147 - D LYS 352	
B GLU 144 - D LYS 313	
A GLU 106 - E ARG 447	
B GLN 139 - D ASN 331	
B GLU 141 - D ARG 302	
B GLU 147 - D LYS 313	
B GLU 144 - D ARG 315	
B GLU 141 - D ARG 315	

POSE #1 - Piper

ANGPTL3-EL	%
B GLU 141 - D ARG 488	
C GLN 137 - D LYS 459	
C GLU 144 - D LYS 459	
A GLU 144 - D ARG 315	
B GLU 141 - D ARG 484	
C GLU 141 - D LYS 459	
C GLU 144 - D ARG 448	
A GLU 147 - D ARG 315	
C GLU 130 - D LYS 313	
A GLU 147 - D ARG 302	
C GLU 130 - D ARG 312	
C ASN 134 - D ARG 312	
C GLU 141 - D LYS 352	
C GLU 147 - D ARG 448	
C GLU 144 - D ARG 450	
C GLU 141 - D ARG 450	

Supplementary figure 11: Average occupancy of all the interactions during MD simulation of the four poses.
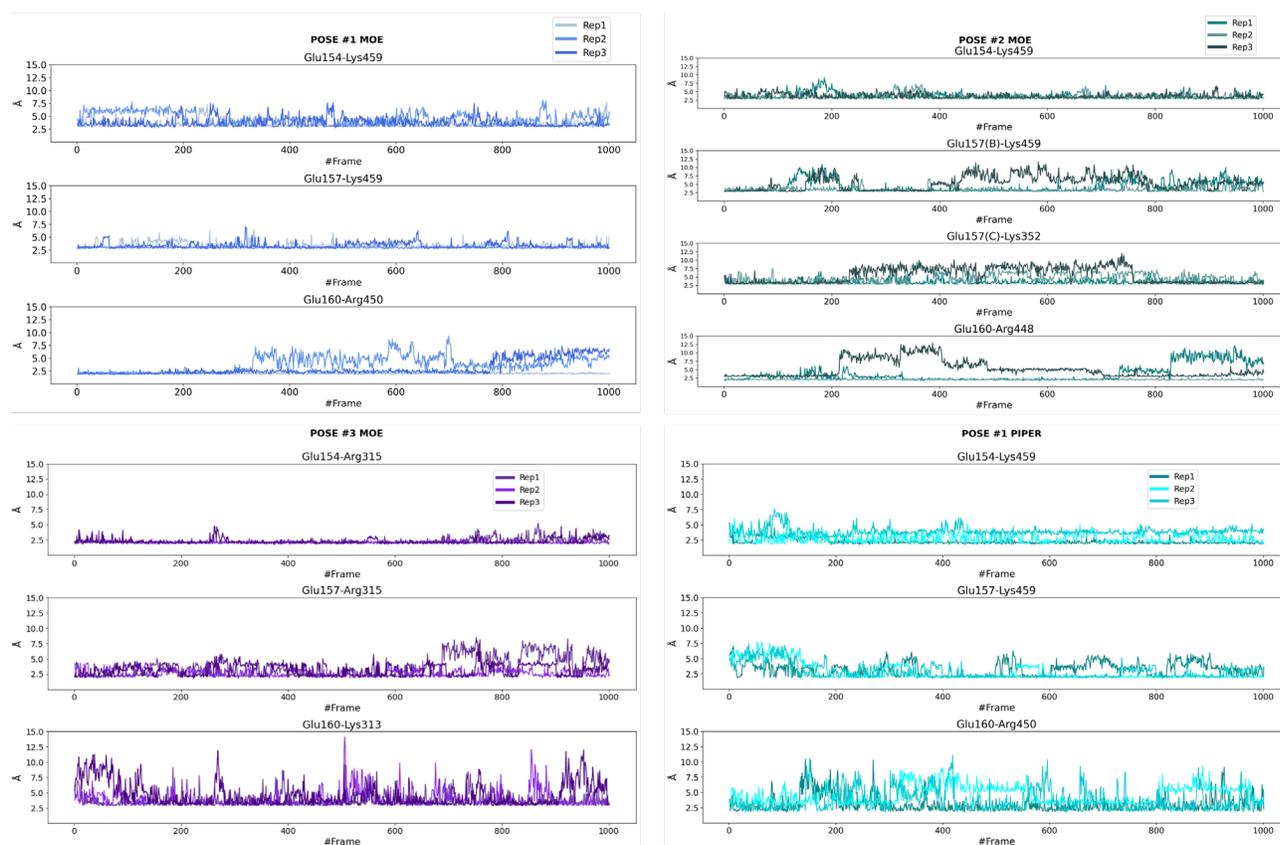
Supplementary figure 12: The minimum distances between ANGPTL3 key residues and the corresponding EL residues are under 5 Å threshold and confirm the presence of interactions for the most simulation time.
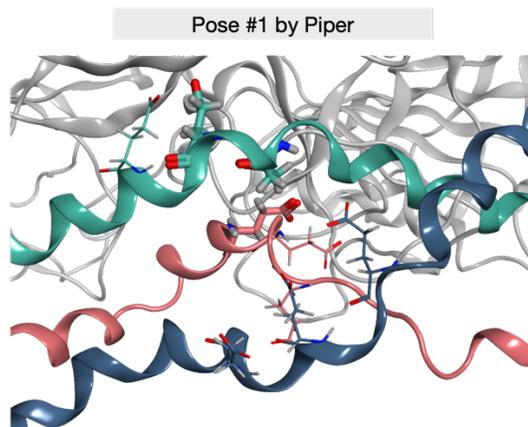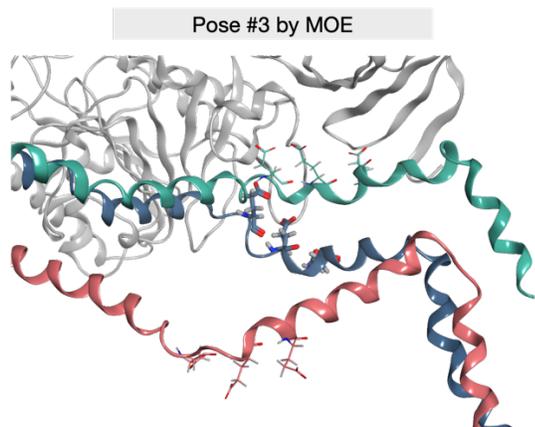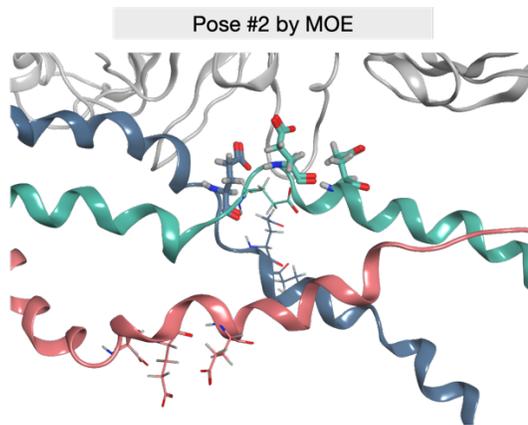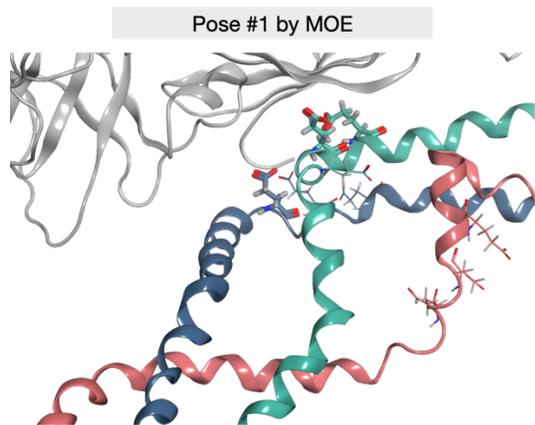
Supplementary figure 13: All Glu154, Glu157 and Glu160 are displayed and colored by chain. The interacting glutamates are bolded. EL is colored in gray.

Simulation	Box sizes (Å)	# of atoms
EL	98x152x76	112160
ANGPTL3 CC 17	149x119x327	567970
ANGPTL3 CC 18	149x119x327	568223
ANGPTL3 CC 19	149x119x327	568067
ANGPTL3 CC 20	149x119x327	568109
EL::ANGPTL3 MOE-1	108x145x314	484744
EL::ANGPTL3 MOE-2	108x145x314	483698
EL::ANGPTL3 MOE-3	108x144x314	484534
EL::ANGPTL3 PIPER	116x134x318	484845

Supplementary table S1: Box sizes and number of atoms for all MD simulations described.